

Phase diagram of vortices in double-layer quantum Hall systems

Igor Tupitsyn,* Mats Wallin, and Anders Rosengren

Department of Theoretical Physics, Royal Institute of Technology, S-100 44 Stockholm, Sweden

(Received 23 August 1994; revised manuscript received 22 May 1995)

We consider the finite-temperature phase diagram of a classical effective model of charged collective vortex excitations in incompressible states with spontaneous interlayer coherence in double layer quantum Hall systems. The phase diagram exhibits surprisingly rich structure, including a Kosterlitz-Thouless transition at high core energy, crystal phases at low core energy, and a variety of transitions between the phases. Our results suggest that alternatives to the expected Kosterlitz-Thouless transition are possible in double layer quantum Hall systems.

Considerable interest has focused on the study of double layer quantum Hall systems (DLQHS), both experimentally¹ and theoretically.² Recent fabrication progress allows experiments to approach a new regime, with interlayer spacing d comparable to the intralayer electron spacing, ultrahigh mobility, and strong interlayer correlations. In this regime, a large variety of phase transitions driven by, for example, thermal fluctuations, or interlayer tunneling, have been predicted by Yang and co-workers.³ These predictions build on recent progress in understanding the nature of charged collective excitations in single layer systems by Sondhi *et al.*⁴ In the limit of small Zeeman energy, the lowest-energy charged excitation is a Skyrmion spin texture, with topological charge (monopole number) $m = \pm 1$, and extra electric charge $Q = \pm \nu e$, where ν is the filling factor. These are connected because the quantized Hall conductance $\sigma_{xy} = \nu e^2/h$ implies that extra flux Φ gives extra charge $Q = \nu e \Phi / \Phi_0$.⁵ In a DLQHS we describe the layer degree of freedom in terms of a pseudospin, which is a spin-1/2 degree of freedom defined as pseudospin up (down) if the electron is in the upper (lower) layer. The real spin is assumed to be frozen out by the magnetic field. The SU(2) pseudospin symmetry in the single layer case is destroyed for finite layer separation, and replaced by U(1) symmetry.⁶ Analogous to the Skyrmion excitations for the $d=0$ case, the low-energy charged collective excitations for $d \neq 0$ are pseudospin textures called merons.⁷ The merons are vortices in the U(1) pseudospin field, carrying vortex charge $s = \pm 1$, and one half unit of topological charge, and thus electric charge $Q = \pm \nu e/2$. The four independent sign choices of s and Q define four meron "flavors." This leads to a picture of thermally excited meron-antimeron pairs, which is expected to have a finite temperature Kosterlitz-Thouless (KT) transition.^{3,6,8} If observed this would be the first example of a finite temperature phase transition in a quantum Hall system. In this paper we present some unexpected alternatives to this prediction.

Statistical mechanics of merons. We study the statistical mechanics of the meron effective action constructed in Ref. 3. Using real-space renormalization and Monte Carlo simulation we construct the finite temperature phase diagram of this model. It is useful to compare with the phase diagram for the two-dimensional (2D) Coulomb gas (for vortices without extra electric charge), which has been determined from renormalization equations⁹ and Monte Carlo simu-

lations.¹⁰ The new feature of the merons is that they are electrically charged, and this turns out to give an unexpectedly rich phase diagram. In the end of the paper we discuss implications for DLQHS.

We define our meron model on a square lattice by the grand partition function Z ,

$$Z = \text{Tr}_{s,q} e^{-\beta H}, \quad (1)$$

$$H = \frac{1}{2} \sum_{i,j} [s_i s_j V^s(r_{ij}) + \alpha q_i q_j V^q(r_{ij})] - \mu N, \quad (2)$$

where s is the vortex charge and q the electric charge, and the trace is over $(s,q)_j = (0,0), \pm(1,\pm 1)$ on all sites j . We are working only at filling factor $\nu=1$ and constrain the net vortex and electric charge of the meron system to be zero. H is the Hamiltonian and $N = \sum |s_i|^2$ is the number of merons. The vortex interaction, $V^s(r) = \ln a/r$, and electric interaction, $V^q(r) = a/r$, are both cut off at the core radius, which sets the lattice spacing a (we will set $a=1$). We use finite lattices of size L^2 with periodic boundary conditions to mimic the thermodynamic limit, and replace the interactions by the corresponding lattice Green's functions: $V^s(r) = 2\pi/L^2 \sum_{\mathbf{k} \neq 0} \exp(i\mathbf{k} \cdot \mathbf{r}) / K^2$, and $V^q(r) = 2\pi/L^2 \sum_{\mathbf{k} \neq 0} \exp(i\mathbf{k} \cdot \mathbf{r}) / K$, where $K^2 \equiv 4 - 2 \cos k_x - 2 \cos k_y$. The $r=0$ terms in the lattice Green's functions will effectively contribute to the chemical potential: $\mu_{\text{total}} = \mu + \mu^s + \mu^q$, where $\mu^s \approx -\pi/4$ and $\mu^q \approx -2\alpha$. The model has three effective parameters, and effective temperature $T = 1/\beta$, the core energy $E_c = -\mu$, where μ is a "chemical potential," and α . We will discuss these in more detail in the end of the paper, but first we consider them as independent input parameters and determine the phase diagram. Note that vorticity and electric charge are coupled only through the constraint that they are attached to the same particle, and that the model is symmetric under $q \rightarrow -q$, interchanging the $(s,q) = \pm(1,1)$ and the $(s,q) = \pm(1,-1)$ meron pairs.

The scaling dimension of the electric interaction, $1/r$, is down by one power of length compared to the logarithmic vortex interaction, $\ln 1/r$. Hence, the electric interaction is expected to be irrelevant at the KT transition, and to essentially only renormalize the meron core energy. To take an approach similar to Kosterlitz real-space renormalization group (RG) for the Coulomb gas,⁸ it is useful to temporarily

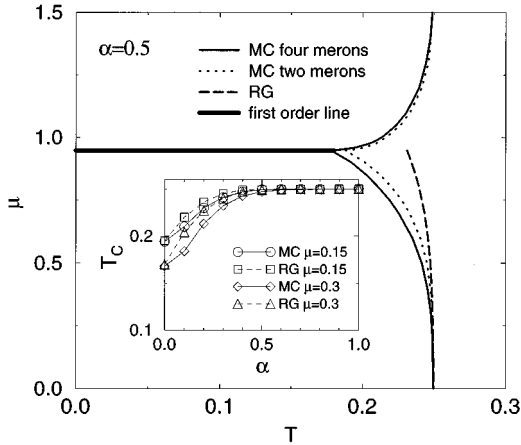


FIG. 1. KT transition lines for $\alpha=0.5$ determined from RG equations, and from MC simulation of the two- and four-meron models. (Ising transition lines are not shown in this plot; see Fig. 2.) Inset: Increase in the KT transition temperature as a function of α , determined from RG equations, and from MC simulation of the four-meron model.

restrict the model from four to only two meron flavors, by keeping, for example, only the $(s,q) = \pm(1,1)$ pairs. The effective interaction cost $V_{\text{eff}}(r)$ to separate a neutral test pair to a distance r , and the correlation function $g(r)$ obey the approximation relations

$$V_{\text{eff}}(r) = \int_a^r \frac{dr'}{\epsilon(r')} \left(\frac{1}{r'} + \frac{\alpha a}{r'^2} \right), \quad (3)$$

$$g(r) = -\frac{2}{a^4} z^2 e^{-V_{\text{eff}}(r)/T}, \quad (4)$$

where $\epsilon(r)$ is a renormalized response function, which we take as

$$\epsilon(r) = 1 - \frac{\pi}{2T} \int_a^r d^2r' r'^2 g(r'), \quad (5)$$

and $z = \exp(\mu/T)$ is the fugacity. These self-consistent equations in terms of renormalized variables, $z(l) = (r/a)^2 z \exp[-V_{\text{eff}}(r)/2T]$, $T(l) = T\epsilon(r)$, where $l = \ln r/a$, yield the RG flow equations

$$\frac{dT^{-1}(l)}{dl} = -\frac{2\pi^2 z^2(l)}{T^2(l)}, \quad (6)$$

$$\frac{dz^2(l)}{dl} = z^2(l) \left[4 - \frac{1 + \alpha e^{-1}}{T(l)} \right]. \quad (7)$$

These equations closely resemble the Kosterlitz equations for the 2D Coulomb gas, with a term added for the electric charge contribution. The KT transition is given by $T_c \epsilon(l \rightarrow \infty) = 1/4$ for all α , since $\alpha e^{-l} \rightarrow 0$. Figure 1 shows the KT critical line from integration of Eqs. (6,7) for $\alpha=0.5$, and the inset shows the dependence of the KT critical temperature on α . Neutral pairs become more strongly confined upon increasing α , which causes the upward shift in T_c .

Equations (6,7) are only expected to be correct in the limit of small fugacity z , i.e., small density. To study the high-

density limit we use Monte Carlo simulation. This also allows us to study the full four-meron model. Our simulation closely follows the simulation of the 2D Coulomb gas by Lee and Teitel.¹⁰ Our MC algorithm consists of attempts to insert near-neighbor neutral pairs of merons on the sites of a square lattice, and the attempts are accepted or rejected according to the usual Metropolis algorithm. We do not use attempts to insert charged pairs, but such composite objects in the system may be formed dynamically in the simulation. Typically 10^5 initial sweeps (a sweep is one update attempt for every site) were discarded for warmup, followed by measurements taken over 10^6 sweeps. Most runs were done on lattices of size 10×10 , 14×14 , and a few runs at 20×20 .

Figure 1 shows MC result for the two- and four-meron models for $\alpha=0.5$, and the KT line from Eqs. (6,7). At small enough chemical potential μ , the results of different determinations of the KT critical line coincide. From improved renormalization equations,⁹ and from MC simulations,¹⁰ it is expected the KT transition in the Coulomb gas is replaced by a first-order transition in the high fugacity limit. This happens in our meron model at the critical value of the chemical potential $\mu_c = \pi/8 + \alpha\pi/\sqrt{8}$, which can be obtained from the Fourier transform of Eq. (2), as for the Coulomb gas.¹⁰ At $\mu > \mu_c$ there is a dense crystal phase [which is not contained in Eqs. (6,7)], which consists of a lattice of merons with both staggered s and q . In this region ‘‘flavor symmetry’’ is spontaneously broken and the four-meron model reduces to the two-meron model, where s and q are no longer independent. The crystal undergoes a Kosterlitz-Thouless transition upon increasing the temperature. The response function (5) measures the stiffness also in the crystal phase, and is used to locate the KT transitions from MC data. At still higher temperature the crystal melts (not shown in Fig. 1; cf. Fig. 2).

Phase diagrams for the four-meron model from MC simulation are shown in Fig. 2. Increasing the temperature further after the upper KT line takes the system into the metallic phase, via either one or two Ising transitions, where the crystal order melts and flavor symmetry is restored. We can define two staggered order parameters for these transitions, one for the vorticity, $M^s = 1/L^2 \langle |\sum_{ij} s(i,j) (-1)^{i+j}| \rangle$, and one for the electric charge, $M^q = 1/L^2 \langle |\sum_{ij} q(i,j) (-1)^{i+j}| \rangle$ [here $i(j)$ denotes the $x(y)$ coordinate]. We locate the critical lines by finite-size scaling, assuming the values of the critical exponents for the 2D Ising model, by locating points where $L^{1/8}M$ becomes independent of system size L . This works quite well for our MC data, indicating that the melting transitions are of Ising type. The four-meron model has separate melting lines for M^s and M^q . In Fig. 2(a) $\alpha=1.5$, and the electric melting temperature is above the vortex melting temperature. In (b) $\alpha=1$, and the melting lines approximately coincide, and in (c) $\alpha=0.5$, the order is reversed. As a simple estimate of the special value α^* where the lines coincide, we determine the free-energy cost to divide the system into two domains separated by a straight wall, which gives $\alpha^* \approx 0.78$. At $\alpha=0$, q will not crystallize. At $\alpha=0.1$ we see in Fig. 2(d) that the q crystal melts inside the vortex crystal phase. Furthermore, the superfluid phase the dissipative metallic state for q is reached *before* the KT transition. This transition is signaled as a sharp drop in the stiffness, Eq. (5), for q . (The

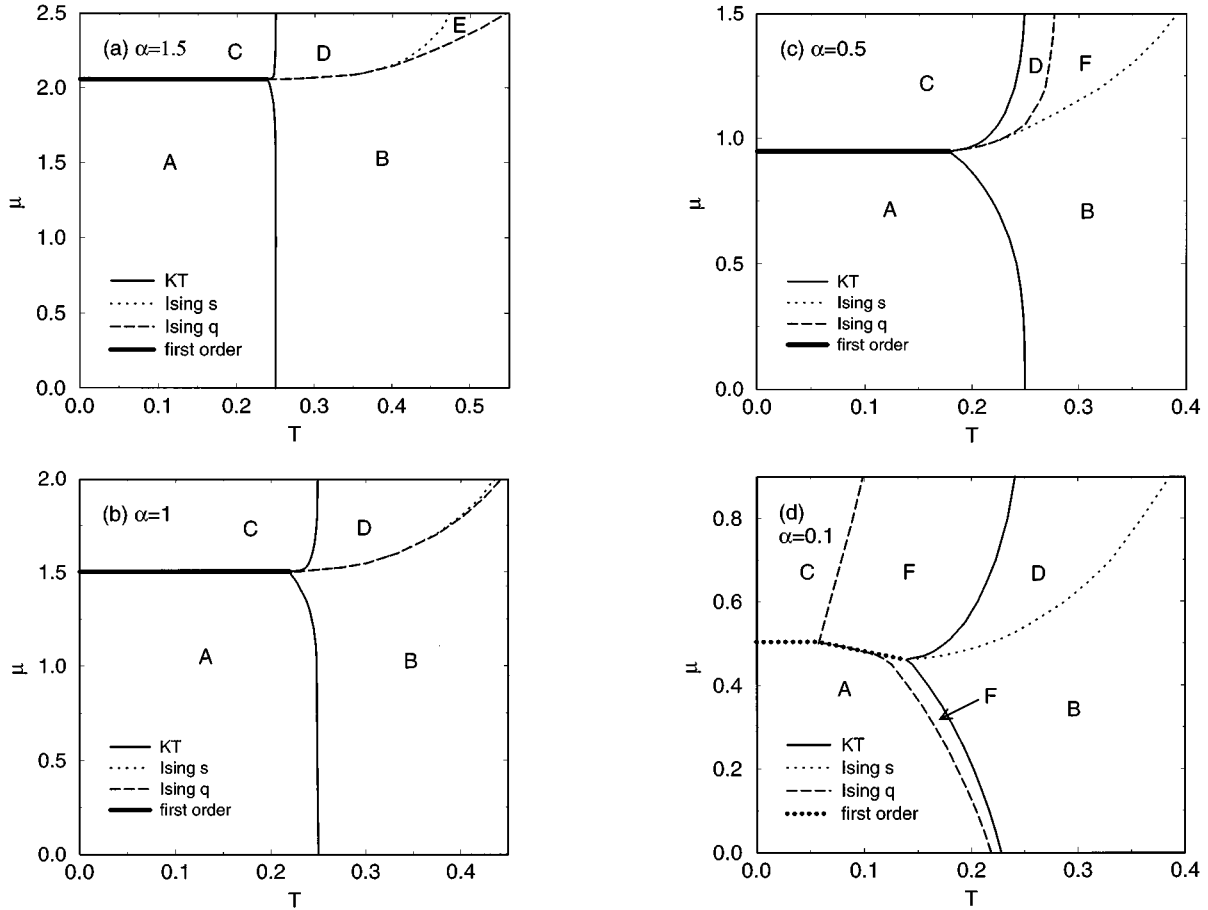


FIG. 2. Phase diagrams constructed from MC simulation of the four-meron model. The phases are (A) meron dipoles (pseudospin superfluid), (B) meron plasma (metallic), (C) meron crystal (insulator), (D) vortex crystal with free defects, (E) vortex plasma, and (F) electric charge plasma.

type of this transition is not clear to us although we call it Ising in the figure.) Hence for sufficiently weakly coupled q dissipation appears already below the KT transition.

Relation to DLQHS. Let us now discuss various approximations involved in our calculation, and the relation of our results to DLQHS systems.

Vortex crystallization in the Coulomb gas case has been considered in superfluid and superconducting films.^{11,12} These are similar to our meron crystals. One has to be careful interpreting these results to physical systems. The square discretization lattice used in our simulations is reasonable for a dilute but not for a dense system. True long-range order (LRO) in a 2D system with continuous symmetry cannot exist at finite temperature according to the Mermin-Wagner theorem. At least we expect LRO to be replaced by quasi-LRO when the discretization lattice is removed, and crystals to be replaced by a dense liquidlike state whose short-range correlations are similar to those of a crystal. This is supported by renormalization calculations for the pure 2D Coulomb gas. Here evidence has been presented for a first-order liquid gas-type transition replacing the KT transition in the high-density limit.⁹ This means that the anticipated KT transition is not the only possibility in these system, and depending on the parameters there might instead be first-order transitions.

Further, we are working within a classical approximation

where all quantum effects are neglected. This is justified for a dilute gas at finite temperature, where quantum effects normally merely renormalize the parameters in the classical action. This assumes that the action correctly captures the order parameter and the low-energy physics. One possible way that this could break down is that the topological objects in the quantum effective action would condense. There is however no reason to suspect that this would happen here, since pairs of merons are fermions, not bosons. For our crystal ground states the effects from quantum fluctuations can be important since they can melt the crystals (see below).

To compare our results with experiments we must translate the effective parameters in our model to physical parameters. If we here denote our effective parameters with overbars we get³ $\bar{\beta} = \beta 2\pi\rho$, $\bar{\beta}\bar{\alpha} = \beta e^2/4\epsilon r_c$, and $\bar{\beta}(E_c + E_c^s + E_c^q) = \beta E_c$, where $\beta = 1/k_B T$ is the physical inverse temperature, ρ the bare pseudospin stiffness, r_c the core radius, and $E_c^s = \pi/4$ and $E_c^q = 2\alpha$ are effective core energy contributions from the periodic lattice potentials.

The Kosterlitz-Thouless transition discussed in this paper has not yet been observed. However, the experiment by Murphy *et al.*¹ has been analyzed within a pseudospin model in Ref. 3, and support has been found for a transition driven by an in-plane magnetic field. The in-plane magnetic field transitions require a finite interlayer tunneling. In contrast, the

zero-field KT transition studied here requires negligible tunneling, because interlayer tunneling breaks the $U(1)$ symmetry and destroys the KT transition. There is reason to believe that such experiments will be possible, since tunneling falls off exponentially with layer separation, whereas the Coulomb interaction that produces the interlayer correlations only falls off like $1/r$.

How would the phase transitions in the obtained phase diagram be observed? A KT transition is signaled in principle by a “universal jump” in the pseudospin stiffness³ as the temperature is tuned through the transition, and a sharp drop in the dissipation for $T < T_c$. The other transitions predicted in our phase diagrams would be visible in thermodynamic quantities, e.g., a first-order transition is signaled by a latent heat.

In a recent Hartree-Fock (HF) calculation by Yang and MacDonald¹³ the regime of layer spacings where the meron picture is valid was estimated. The core energies in the HF approximation, translated to our effective core energy, are inside our crystal state, i.e., $E_c^{\text{HF}} < E_c^{\text{crystal}}$. This may however depend on uncertainties in details of the translation between the different calculations (such as precisely how to define the meron core, etc.). HF has a crystal ground state at low core

energy, but this is not expected to be the true ground state, which is instead believed to be a charge density wave. Thus if our crystal state can be identified with the HF crystal, it is not expected to appear.

In summary, we have studied the finite temperature statistical mechanics of an effective classical meron model motivated by recent progress in understanding the nature of charged excitations in DLQHS. We find an unexpectedly rich phase diagram containing, e.g., meron crystals for low core energy. Our results demonstrate that the previously anticipated Kosterlitz-Thouless transition is not the only possible outcome of experiments on DLQHS, but one might instead get a first-order transition. However, a more detailed analysis than the one presented here is needed to establish to what extent our results actually apply to DLQHS. This adds motivation to further experimental study of DLQHS, and also to look for other systems described by our model.

We thank Steven Girvin and Kun Yang for very stimulating and helpful discussions. This work was supported by the Swedish Natural Science Research Council and by the Swedish Institute.

*Permanent address: Institute of Superconductivity and Solid State Physics, Kurchatov Institute, 14 Kurchatov Square, 123182 Moscow, Russia.

¹Y. W. Suen *et al.*, Phys. Rev. Lett. **68**, 1379 (1992); J. P. Eisenstein *et al.*, *ibid.* **68**, 1383 (1992); S. Q. Murphy, J. P. Eisenstein, G. S. Boebinger, L. N. Pfeiffer, and K. W. West, *ibid.* **72**, 728 (1994).

²B. I. Halperin, Helv. Phys. Acta **56**, 75 (1983); T. Chakraborty and P. Pietiläinen, Phys. Rev. Lett. **59**, 2784 (1987); E. H. Rezayi and F. D. M. Haldane, Bull. Am. Phys. Soc. **32**, 892 (1987); A. H. MacDonald, Surf. Sci. **229**, 1 (1990); Z. F. Ezawa and A. Iwazaki, Int. J. Mod. Phys. B **19**, 3205 (1992); Phys. Rev. B **47**, 7295 (1993); **48**, 15 189 (1993); Song He, S. Das Sarma, and X. C. Xie, *ibid.* **47**, 4394 (1993).

³K. Yang, K. Moon, L. Zheng, A. H. MacDonald, S. M. Girvin, D. Yoshioka, and S.-C. Zhang, Phys. Rev. Lett. **72**, 732 (1994); K. Moon, H. Mori, K. Yang, S. M. Girvin, A. H. MacDonald, L. Zheng, D. Yoshioka, and S.-C. Zhang, Phys. Rev. B **51**,

5138 (1995).

⁴S. L. Sondhi, A. Karlhede, S. A. Kivelson, and E. H. Rezayi, Phys. Rev. B **47**, 16 419 (1993).

⁵K. Yang, L. K. Warman, and S. M. Girvin, Phys. Rev. Lett. **70**, 2641 (1993).

⁶X. G. Wen and A. Zee, Phys. Rev. Lett. **69**, 1811 (1992); Phys. Rev. B **47**, 2265 (1993).

⁷I. Affleck, Phys. Rev. Lett. **56**, 408 (1986).

⁸V. L. Berezinskii, Zh. Eksp. Teor. Fiz. **61**, 1144 (1971) [Sov. Phys. JETP **34**, 610 (1972)]; J. M. Kosterlitz and D. J. Thouless, J. Phys. C **5**, L124 (1972); **6**, 1181 (1973).

⁹P. Minnhagen and M. Wallin, Phys. Rev. B **40**, 5109 (1989).

¹⁰J.-R. Lee and S. Teitel, Phys. Rev. Lett. **64**, 1483 (1990); Phys. Rev. B **46**, 3247 (1992).

¹¹M. Gabay and A. Kapitulnik, Phys. Rev. Lett. **71**, 2138 (1993).

¹²S.-C. Zhang, Phys. Rev. Lett. **71**, 2142 (1993).

¹³K. Yang and A. H. MacDonald, Phys. Rev. B **51**, 17 247 (1995).